Low-energy K^--nucleon potentials and the nature of the $\Lambda(1405)$

P. B. Siegel* and W. Weise
Institute of Theoretical Physics, University of Regensburg, D-8400 Regensburg, Federal Republic of Germany
(Received 15 April 1988)

The low-energy $\bar{K}N$ system is examined using a general separable and a vector-meson exchange potential. A direct fit to the data including the K^-p threshold branching ratios is made in order to determine the nature of the resonance at 1405 MeV. Satisfactory fits are obtained using potential parameters within the range of expected SU(3) breaking and vertex coupling constants roughly consistent with values derived from NN analyses.

I. INTRODUCTION

There are some controversial problems concerning the $\bar{K}N$ system ($K^-p, \bar{K}^0n$) at low energies. One deals with the nature of the resonance at 1405 MeV [the $\Lambda(1405)$], and another one with the disagreement between K^-N scattering lengths extracted from scattering data and the atomic level shift (see Ref. 1 for a detailed discussion). With respect to the $\Lambda(1405)$, its description as a three-quark s-channel resonance, a quasibound $\bar{K}N$ system, or a combination of these two states still remains unclear. Although there has been much work done in trying to understand this system,[1] these puzzles still persist. In this paper, we apply various potential models to the $\bar{K}N$ system at low energies. We examine the situation with respect to the degree of SU(3) symmetry breaking needed to fit the data as well as a comparison with potential parameters derived from NN scattering. We concentrate on the energy region between 1400 and 1460 MeV in which there are three types of available information: (a) the Σ-π mass spectrum centered at 1405 MeV, (b) the K^-p atomic $1s$ level shift and branching ratios at threshold, and (c) the low-energy scattering data.

The usual approaches for fitting the data are of two types: K-matrix parametrizations with dispersion relation constraints[2,3] and potential models.[4,5] The K-matrix approaches fit the low-energy scattering data, the threshold branching ratios, and the resonance at 1405 MeV very well with parameters which vary slowly with energy. These results, however, predict a value for the $1s$ atomic level shift which has a sign opposite to the experimental result. Attempts have been made with marginal success to reconcile this difference by considering anomalous Coulomb corrections[6] as well as Coulomb-nuclear interference effects.[7] Also, the K-matrix formalism is not equipped to unambiguously reveal the character of the $\Lambda(1405)$ resonance.[8]

Potential models have also been used in fitting the low-energy data. This approach has the advantage of offering an energy dependence for the amplitudes which incorporates the dynamics of the system. In addition, potential models can incorporate and differentiate between an s-channel (three-quark state) and a t-channel (quasibound-state resonance) situation within a physical model. The disadvantages include model dependencies and a limited range of validity. Nonetheless, these models offer some "physics" to the parametrization and a scheme for extending the amplitudes off shell.

One of the first potential models applied to the $\bar{K}N$ system was that of Alberg *et al.*,[4] who matched separable potential parameters to the amplitudes of the available K-matrix analysis. Other potential models have been constructed to fit the data directly.[9] The low-energy scattering data, the resonance at 1405 MeV, and even the threshold value for the $2p$-$1s$ atomic level shift (with some difficulty) have been incorporated to fit within simple potential models.[7,9] In particular, there has been a lot of effort to obtain a scattering length in agreement with the experimental level shift. We emphasize here that this is not the only available data at threshold. The threshold branching ratio data of Refs. 10 and 11 place tight constraints on the amplitudes and on the potential coupling strengths. In addition, the branching ratio data sets are self-consistent and have smaller errors than the atomic level shift data. This data is included in the K-matrix parametrizations, and consequently in the potential fits of Refs. 4 and 5. It is not included, however, in recent potential model fits to the data of Refs. 7 and 9, which perform computational gymnastics to find compatibility with only the atomic level shift results and the scattering and resonance data.

In this paper we examine a class of potential forms for the low-energy $\bar{K}N$ system. We fit directly to the data. We also emphasize that there is sufficient low-energy data to put tight constraints on any potential model. Two different types of potentials will be considered: a separable potential in momentum space and a local potential (simple meson exchange) in coordinate space, both of which will be guided initially by SU(3) symmetry considerations. In the next two sections the framework will be discussed, and in Secs. IV and V the results will be presented. We are limiting our consideration to the strangeness $S=-1$ sector (i.e., we do not include the K_L^0p scattering data).

II. THE POTENTIAL PARAMETRIZATION

In this section we describe the potential parametrization and the framework in which the scattering amplitudes are calculated. We will be fitting to data in three

different energy regions, and these will be referred to as resonance, threshold, and scattering data. The resonance data consist of the Σ-π spectrum centered at 1405 MeV, which is below the K^-p threshold [i.e., the $\Lambda(1405)$ resonance]. The threshold data which we fit to will be the decay branching ratios of the K^-p atom. These are defined as

$$\gamma=\frac{\text{rate}(K^-p\to\Sigma^-\pi^+)}{\text{rate}(K^-p\to\Sigma^+\pi^-)}\ , \tag{1}$$

$$R_c=\frac{\text{rate}(K^-p\to\text{charged particles})}{\text{rate}(K^-p\to\text{all final states})}\ , \tag{2}$$

and

$$R_n\equiv\frac{\text{rate}(K^-p\to\pi^0\Lambda)}{\text{rate}(K^-p\to\text{all neutral states})}\ . \tag{3}$$

We do not fit to the atomic level shift initially, but will examine the $1s$ energy shift resulting from the branching ratio fit. The scattering data consist of recent low-energy elastic and reaction data for $P_{\text{lab}}<200$ MeV/c from Refs. 12–15. There are 48 data points. For the resonance and scattering data an isospin basis will suffice. However, the threshold branching ratios are very sensitive to isospin breaking effects[16] due to the mass difference between the K^-p and $\bar{K}^0n$ systems, causing a rapid energy dependence between the two thresholds. To handle these effects, one can either solve for the K matrices of the respective isospin channels and apply the isospin breaking corrections of Dalitz and Tuan,[16] or solve the six-channel problem in the particle basis. Here we take the latter approach since it is easier for our application. The threshold branching ratios are not particularly sensitive to the inclusion or exclusion of the Coulomb potential.[17]

We consider two forms for the potentials, a simple separable potential and a local potential. In both cases, the relative couplings between the channels are guided by SU(3) symmetry properties. The separable potential is solved in momentum space, which facilitates the calculation, and the local potential in coordinate space. In both cases we will seek solutions which do not stray too far from these guiding SU(3) properties. We use the coupled-channel potential model with nonrelativistic propagators (or dynamics) as our mathematical framework for solving for the scattering amplitudes. Later we show that for the separable potential similar results are obtained by using a relativistic propagator. The coupled equations are written in coordinate space as

$$\nabla^2\Psi_i(r)+k_i^2\Psi_i(r)-2\mu_i\int V_{ij}(r,r')\Psi_j(r')d^3r'=0 \tag{4}$$

where $\Psi_i(r)$ represents the wave function and μ_i is the reduced energy for channel i. The six channels relevant for our problem are the $\Sigma^+\pi^-$, $\Sigma^0\pi^0$, $\Sigma^-\pi^+$, $\Lambda\pi^0$, K^-p, and $\bar{K}^0n$, and will be referred to as channels 1–6, respectively. The center-of-mass momenta k_i of channel i are determined from the total energy E:

$$k_i^2=[E^2-(m_i-M_i)^2][E^2-(m_i+M_i)^2]/(4E^2)\ , \tag{5}$$

where m_i and M_i represent the meson and baryon masses for channel i.

For the separable potential we use the following ansatz:

$$V_{ij}(k,k')=\frac{g^2}{4\pi}C_{ij}v_i(k)v_j(k')$$

$$=\frac{g^2}{4\pi}C_{ij}\frac{\alpha_i}{\alpha_i^2+k^2}\frac{\alpha_j}{\alpha_j^2+k'^2}\ . \tag{6}$$

Using this separable form and the nonrelativistic propagator the problem of solving the coupled channel equations is algebraic (see Appendix A). A key ingredient in the solution is the evaluation of the integral I_i defined as

$$I_i\equiv\int\frac{2\mu_i v_i^2(p)p^2dp}{k_i^2-p^2+i\epsilon}\ . \tag{7}$$

If $v_i(p)$ has the simple form as in Eq. (6) then the integral is easily solved analytically with the result given in Appendix A. The solution to the six coupled equations is readily done, and a search on the potential parameters is feasible. This approach is essentially a particular form of a K-matrix parametrization which tries to include the dynamics of the six-channel system. Previous potential parameter searches on the data[7,9] have used complex components to represent the Λ-π channel. Here we include this channel explicitly in order to incorporate the threshold branching ratio data.

It has been pointed out[9] that one should use a relativistic propagator in dealing with this system with a separable potential model, the point being that although the $\bar{K}N$ system is at nonrelativistic energies, the Σ-π and the Λ-π systems are not. We find that in the energy range considered here between 1400 and 1460 MeV there is no loss of accuracy by using a nonrelativistic propagator. This is demonstrated in Fig. 1. The difference between using a relativistic versus a nonrelativistic propagator would occur in the denominator of the integral in Eq. (7) with the replacement of k^2-p^2 by $E-(m_i^2+p^2)^{1/2}-(m_j^2+p^2)^{1/2}$. In both cases the "pole" piece is the same and is given by $i\pi\mu kv^2(k)$. Only the principle value pieces will differ, but they can be made roughly equal by an appropriate choice of off-shell range. In Fig. 1 we show this comparison. The solid curves correspond to a nonrelativistic range parameter α of 1 GeV/c for the three channels. At any particular energy there exists a corresponding relativistic range which will produce the same principle value integral. The dashed lines correspond to relativistic ranges which give equivalent principle values with α between 690 and 830 MeV. The energy dependence of the two forms will differ, but over the small energy range considered here the difference is less than 10%. These ranges for α were roughly what was needed to fit the data with the separable potential. For ranges $200<\alpha<1500$ MeV similar small deviations were found. For the $\bar{K}N$ system in particular there is essentially none. Therefore, for any set of nonrelativistic ranges there exists a set of relativistic ranges which will give similar results. (This argument was tested only for these small energy regions and for the separable potential forms.)

We also consider a local potential. The specific form,

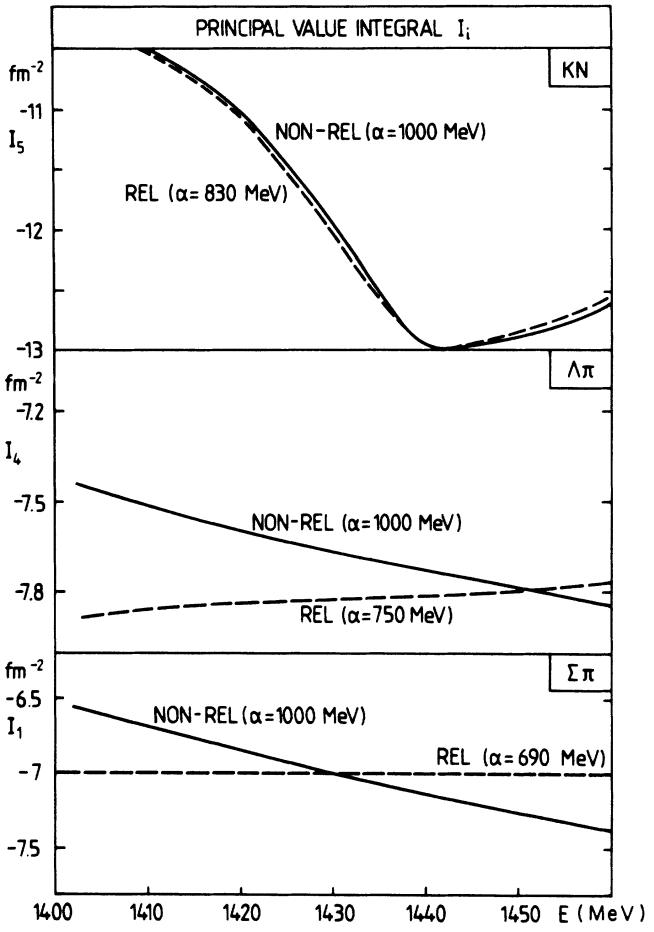

FIG. 1. The principle value integral I_i of Eq. (7) is plotted as a function of total energy E for the K-N channel, the π-Λ channel, and the π-Σ channel. The off-shell ranges, α_i, for the separable potentials used [Eq. (6)] are given in parentheses for the nonrelativistic propagator $(K^2-p^2)^{-1}$ and for the relativistic propagator $[E-(m_i^2+p^2)^{1/2}-(m_j^2+p^2)^{1/2}]^{-1}$.

derived in Appendix B, is motivated by a simple vector-meson exchange picture of the interaction. The q^2 dependence is given by

$$V_{ij}(q^2)=\frac{g_{ij}\left[g_{ij}^V-g_{ij}^T\frac{q^2}{4M^2}\right]}{q^2+m^2}\left[\frac{\alpha^2-m^2}{\alpha^2+q^2}\right]. \quad (8)$$

The parameter m corresponds to the mass of the exchanged meson, and the range parameter α to the form factor of the baryon-baryon-(vector-meson) vertex. The parameter g_{ij} is the meson-meson-(vector-meson) vertex coupling constant; g_{ij}^V and g_{ij}^T are the various baryon-baryon-(vector-meson) vector and tensor vertex coupling constants, respectively. For this local interaction, the Coulomb potential was added in the (K^-p) channel, and caused an increase in the $\Sigma\pi$ production $(K^-p\to\Sigma\pi)$ of 10 percent for the data points at $T_{\rm lab}=70$ MeV.

III. GENERAL CONSIDERATIONS

For the low-energy data considered here, the s-wave amplitudes dominate (p wave contributing only 5 percent at the highest energy of 1460 MeV), and we confine our analysis to this partial wave. The form of the potentials gives three types of parameter variations; the relative coupling strengths C_{ij} [see Eq. (6)], the overall strength g, and the off-shell ranges. Our general procedure for searching on the parameters for the separable potential will be to fix the ranges and couplings C_{ij} and adjust the strength g so that a resonance state is formed at 1405 MeV. The chi squared for the scattering and branching ratio data is then calculated.

The scattering amplitudes for the various channels are quite sensitive to the coupling constants C_{ij}, and we begin our search on these parameters with the guidance of models based on the SU(3) symmetry of the KN system. The cloudy-bag model[18] has been successfully applied to the K^-N low-energy scattering data and the $\Lambda(1405)$ resonance. The original Lagrangian is based on chiral SU(3)×SU(3) symmetry. A local chiral rotation generates a four point meson-quark contact interaction in the s-wave channel. When this contact potential is projected onto baryonic states the resulting relative coupling strengths between the channels are given by[18]

$$(C_{ij}^0)=\begin{bmatrix} -2 & -\frac{\sqrt{6}}{4} \\ -\frac{\sqrt{6}}{4} & -\frac{3}{2} \end{bmatrix} \text{ (for isospin } I=0), \quad (9a)$$

where $i=1,2$ refers to the $\Sigma\pi$ and $\bar{K}N$ channels, and

$$(C_{ij}^1)=\begin{bmatrix} -1 & 0 & -\frac{1}{2} \\ 0 & 0 & \frac{\sqrt{6}}{4} \\ -\frac{1}{2} & \frac{\sqrt{6}}{4} & -\frac{1}{2} \end{bmatrix} \text{ (for isospin } I=1), \quad (9b)$$

where $i=1,2,3$ refers to the $\Sigma\pi$, $\Lambda\pi$, and $\bar{K}N$ channels, respectively.

These same relative coupling strengths result if one assumes a simple vector-meson exchange picture with universal coupling for all the vertices.[19] Due to the success of the former model and the expected approximate validity of SU(3) symmetry we start our searches with the above values for the C_{ij}'s. We initially introduce SU(3) breaking by using different masses for the respective channels. With these assumptions, the interactions depend on only two parameters, an overall strength g and the common range parameter α in Eq. (6) [alternatively, the mass parameter m in Eq. (8)]. We initially take $\alpha=\infty$ in Eq. (8).

The results obtained with these simple forms are presented in Fig. 2(a) for the separable potential, and in Fig. 2(b) for the local potential. The solid line corresponds to values of the strength and range for which a K^-p resonance is formed at 1405 MeV. The dashed line corresponds to combinations of strength and range which reproduce the experimental branching ratio γ at threshold [see Eq. (1)]. It is interesting to note that the other

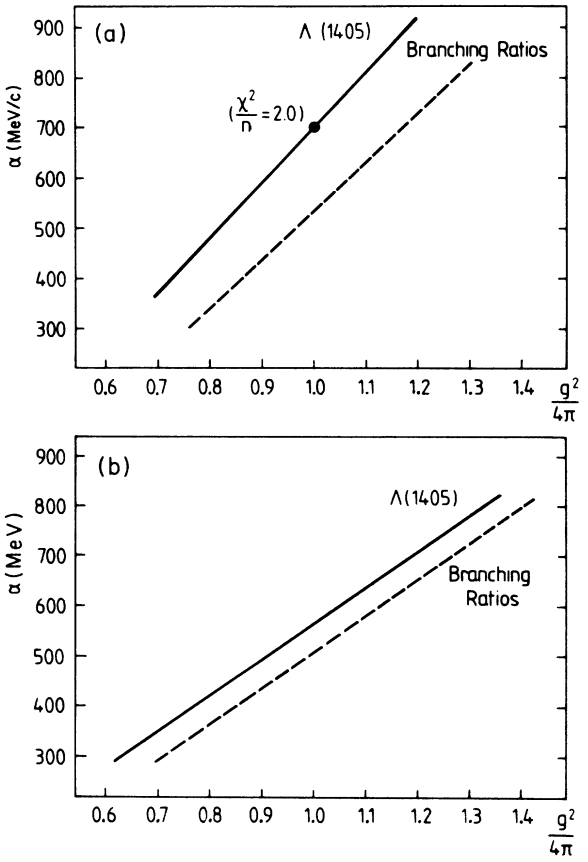

FIG. 2. The solid lines correspond to combinations of strength and range which produce a quasi-bound-state resonance at 1405 MeV. The dashed lines correspond to combinations of the parameters which reproduce the experimental branching ratio γ. In (a) the separable potential of Eq. (6) (with $\alpha_i=\alpha_j$) is used, and in (b), we use the local potential of Eq. (8) (with $g_T=0$ and $\alpha=\infty$, and $g^2=g_{ij}g_{ij}^V$).

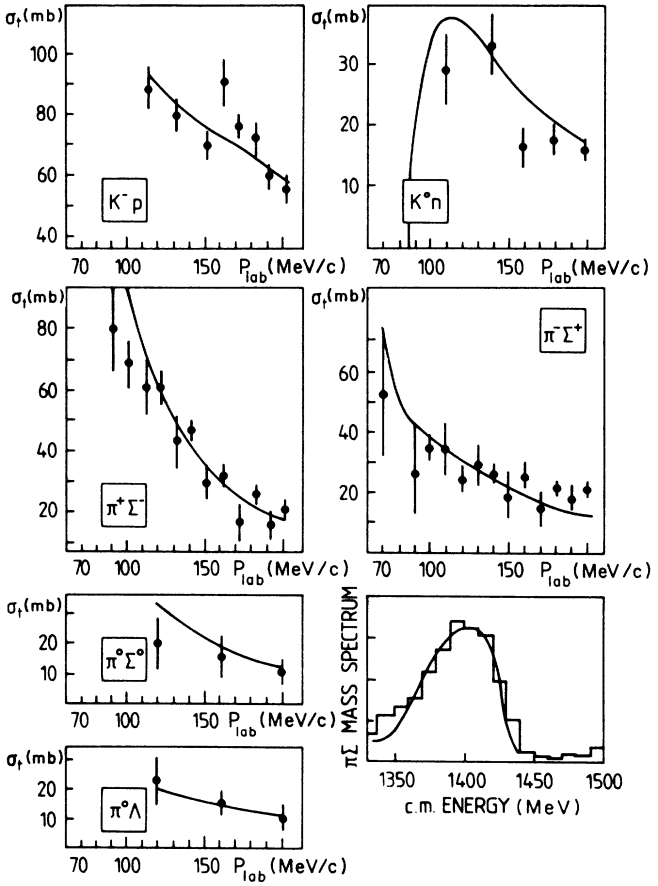

FIG. 3. Comparison with the low-energy data taken from Refs. 12–15 and 20 using the potential of Fig. 2(a) with $\alpha=700$ MeV/c and $g^2/4\pi=1.0$.

two branching ratios are very close to the experimental values as well.[17] The results for the two potential forms are qualitatively similar. The point in Fig. 2(a) corresponds to a value of $\chi^2=2.0$ for the scattering data. The resulting cross sections for these optimal values of the parameters α and g of the separable potential are shown in Fig. 3 along with the theoretical $\Sigma\pi$ mass spectrum ($k_{\text{c.m.}}\times|\,\Sigma\pi$ elastic scattering amplitude $|^2$) normalized to the $\Sigma\pi$ mass spectrum data of Hemingway;[20] we note that the shape of the $\Sigma\pi$ mass spectrum agrees well with Ref. 20. These results should be seen together with the branching ratios listed in Table I. These curves are very similar to those of Fig. 9 in Ref. 18. This is not surprising, since the resulting potential in the cloudy-bag model is almost separable and depends on two parameters. Our results here for the potential form of Eq. (6) should be similar to those of Ref. 18, with perhaps a different mean-

TABLE I. Calculated threshold branching ratios $\gamma=\text{rate}(K^-p\to\Sigma^-\pi^+)/\text{rate}(K^-p\to\Sigma^+\pi^-)$, $R_c\equiv\text{rate}(K^-p\to\text{charged particles})/\text{rate}(K^-p\to\text{all final states})$, $R_n\equiv\text{rate}(K^-p\to\pi^0\Lambda)/\text{rate}(K^-p\to\text{all neutral states})$, using (a) separable potential [cf. Figs. 3 and 2(a)]; (b) separable potential plus s-channel resonance at $M_0=1430$ MeV (cf. Fig. 4); (c) meson-exchange potential (cf. Fig. 5). The experimental values are shown for comparison.

	K^-p threshold branching ratios			
	Separable potential	Separable potential +s-channel resonance	Meson-exchange potential	Expt.
γ	1.21	2.34	2.34	2.36±0.04
R_c	0.65	0.64	0.66	0.664±0.011
R_n	0.12	0.22	0.14	0.189±0.015

ing for the parameters. We note that this good agreement does not hold for the branching ratios. We were unable to fit all three sets of data with only these two parameters.

In the next section we examine how much SU(3) symmetry breaking in the potential is necessary to obtain satisfactory fits to all the data. We will also investigate whether the explicit additional inclusion of an s-channel resonance is necessary and compatible with the data. Finally coupling constants for an effective vector-meson exchange model will be determined.

IV. RESULTS FOR SEPARABLE POTENTIALS

There are many possible ways in which to break SU(3) symmetry in the coupling potential. The coupling constants between the various channels can be varied as well as the ranges. It is, however, difficult to make a direct connection with flavor SU(3) or chiral SU(3)×SU(3) breaking terms of a fundamental Lagrangian, since the inclusion of form factors "mock up" vertex renormalizations. Although these renormalizations are supposed to be small for appropriate ranges,[18] here we wish to show that, for ranges commensurate with the size of the meson-baryon system, a fit to all the data is possible within 25 percent of the SU(3)-derived C_{ij} coefficients. We will consider a $\chi^2/(\text{data point}) > 3.0$ as an unacceptable fit since a $\chi^2/(\text{data point}) < 1.8$ was possible by searching on six parameters of an appropriate choice.

First, the range parameters α_i were varied. An acceptable fit to the data was not found. Next, the coupling coefficients were modified according to the ansatz $C'_{ij} = f_i f_j C_{ij}$. In this parametrization, the f_i's represent vertex corrections in the particle basis; this is, the same correction for the $I=0$ and $I=1$ channels. The six parameters f_i and α_i were varied without finding an acceptable fit.

A successful scheme is the free variation of the C_{ij} for a fixed range α. This type of freedom is incorporated in K-matrix fits. Here we wish to investigate how much variation from the values in Eq. (9) is necessary. We quantify this deviation by multiplying the C_{ij}'s by a factor f_{ij} and search for a fit which minimizes the SU(3) breaking. A solution was found in which only a 15 percent variation (i.e., $0.85 < f_{ij} < 1.15$) of the coefficients $C^0_{11}f^0_{11}$, $C^0_{12}f^0_{12}$, $C^0_{22}f^0_{22}$, $C^1_{11}f^1_{11}$, $C^1_{13}f^1_{13}$, and $C^1_{33}f^1_{33}$ from the values of Eq. (9) produced a $\chi^2/(\text{data point}) = 1.8$. The respective modification factors f_{ij} for this best fit are 0.85, 0.85, 1.02, 1.15, 1.15, and 0.85 with $\alpha = 800$ MeV/c. We note that restricting $0.9 < f_{ij} < 1.1$ produced a best $\chi^2/(\text{data point})$ of 3.7 for 200 MeV/c $< \alpha <$ 2 GeV/c. Variational schemes which vary the ranges as well as the C_{ij} are possible as well. A 15 percent variation of the potential strengths translates to only a 7.5 percent renormalization of the vertices. One peculiar aspect of the above fit is that $f_{12}(I=0) = 0.85$, whereas $f_{13}(I=1) = 1.15$. In a particle basis, this corresponds to a strong potential for the double charge exchange reaction $K^-p \to \pi^+\Sigma^-$, which is not allowed by either single vector-meson or quark exchange. If this direct potential is not permitted, then larger breaking of SU(3) is required for a fit to the data. With this restriction, a $\chi^2(\text{data point}) = 1.6$ was found for $\alpha = 600$ MeV/c and respective modification factors f_{ij}: 0.76, 1.26, 1.07, 0.76, 1.26, 0.78, which correspond to roughly 25 percent SU(3) breaking. It would be interesting to see if the cloudy-bag model would be flexible enough to renormalize the vertices to simultaneously fit the branching ratio data as well as the scattering and resonance data, which are so well reproduced.

The inclusion of an "elementary" s-channel resonance was considered by the addition of a potential in the $I=0$ channel of the form

$$V^0_{ij}(k,k') = \frac{g_i g_j}{4\pi} \frac{M_0}{E - M_0} \frac{\alpha_i}{\alpha_i^2 + k^2} \frac{\alpha_j}{\alpha_j^2 + k'^2} \tag{10}$$

where M_0 is this mass of this s-channel resonance. Such a resonance could be interpreted as a three-quark SU(3) singlet state which is believed to exist and is often associated with the resonance at 1405 MeV but with notorious problems to reproduce this mass in naive valence quark models. As a requirement for a particle resonance we restrict $\det(V_{ij}) = 0$, which determines the form in Eq. (10) for the relative couplings. When this potential is added to that of Eq. (6), an excellent fit of all the data is obtained, but only for very weak resonance coupling param-

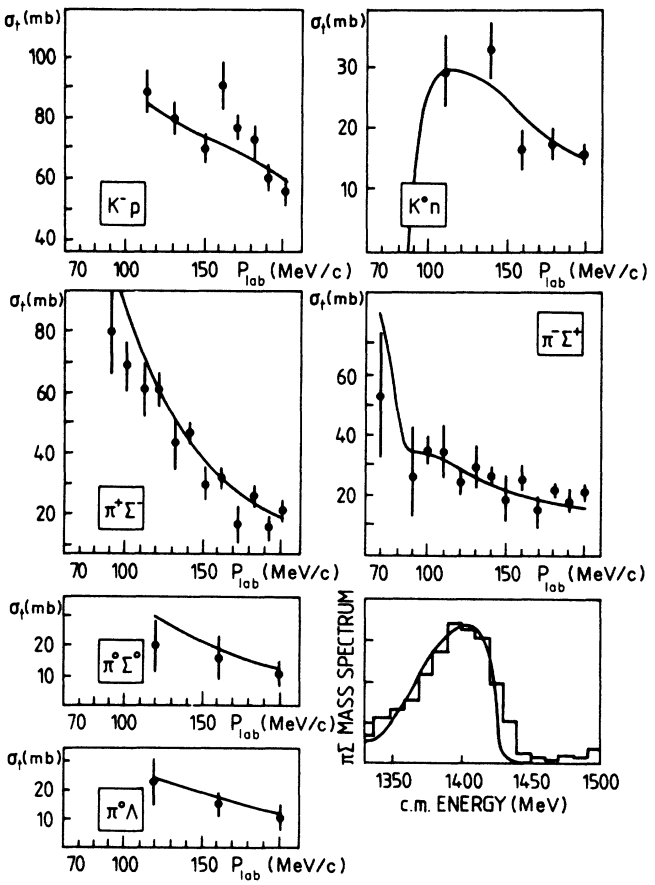

FIG. 4. Comparison with the low-energy data using a potential which is the sum of the potential in Eq. (6) and the s-channel resonance form in Eq. (10).

eters $g_i g_j$ and for $1430 < M_0 < 1432$ MeV. The effect of this potential is to shift the dashed line of Fig. 2(a) over to the solid line. This potential, however, adds another resonance to the one produced (as a bound-state-type resonance) from the potential of Eq. (6). So as not to spoil the Σ-π mass spectrum, the location of this second resonance needs to be close to the $K^- p$ threshold and of very weak coupling. An excellent fit, shown in Fig. 4, was obtained for values of $g_1^2/(4\pi)=(\frac{3}{2})^2 g_2^2/(4\pi)=0.07$. A similar rapid energy dependence near threshold of the amplitudes was suggested in Ref. 21 in order to explain the $K^- p$ atomic data. In our analysis it also produces good agreement with the branching ratio data (see Table I). A very weak coupling to this $\Lambda(J=\frac{1}{2}^-)$ three-quark state would be quite peculiar, since its spin-orbit partner, $\Lambda(J=\frac{3}{2}^-)$, at 1520 MeV is coupled strongly to the KN system. It would be very difficult to verify this second resonance just below threshold by other experimental means. We mention it here since it is a fit which respects SU(3) symmetry to all the data. Attempts to incorporate this s-channel potential with stronger couplings to fit the data were unsuccessful.

V. MESON-EXCHANGE POTENTIAL

As a second potential model we consider a simple vector-meson exchange interaction generated by the Hamiltonian

$$
\begin{aligned}
H_{\rm int} = {} & \tfrac{1}{2} g_{\rm PPV}[\rho_\mu\cdot(\pi\times\partial^\mu\pi)+i\rho_\mu\cdot K^\dagger\tau\partial^\mu K + iK_\mu^{*\dagger}\tau K\cdot\partial^\mu\pi+\sqrt{3}i\omega_8^\mu K^\dagger\partial_\mu K] \\
& + \frac{1}{2}\left[\rho_\mu\cdot N\tau\left(g^V_{\rho NN}\gamma^\mu + g^T_{\rho NN}\frac{i\sigma^{\mu\nu}}{2M}q_\nu\right)N + g_{\rho\Sigma\Sigma}\rho_\mu\cdot(\bar{\Sigma}\gamma^\mu\times\Sigma) + g_{K^*N\Sigma}(\bar{N}\tau K_\mu^*\gamma^\mu\cdot\Sigma+\bar{\Sigma}\cdot\gamma^\mu K_\mu^{*\dagger}\tau N)\right. \\
& \left. + g_{K^*N\Lambda}(\bar{N}K_\mu^*\gamma^\mu\Lambda + K_\mu^{*\dagger}\bar{\Lambda}\gamma^\mu N) + g_{\omega_8 NN}\bar{N}\gamma_\mu N\omega_8^\mu\right] . \qquad (11)
\end{aligned}
$$

Initially only potentials representing single ρ, ω_8, and K^* exchange are considered, where ω_8 corresponds to the pure octet state ($\omega_8=\sqrt{2/3}\omega+\sqrt{1/3}\phi$). In Appendix B the forms for the local nonrelativistic reduction of these meson-exchange potentials [Eq. (B3)] are given. For simplicity we assume that the meson-meson-(vector-meson) (PPV) coupling constants are related by SU(3) symmetry with the overall scale fixed by $g_{\rho\pi\pi}$ determined from the width of the ρ decay. This condition sets $g_{\rm PPV}\simeq 6$. Also, to limit the number of parameters, a tensor coupling is included only at the ρNN vertex, where $g_T/g_V\simeq 6$, and not at the ωNN vertex, where g_T is approximately zero from NN analysis. The other tensor couplings are less well determined. An additional form factor parameter α is also introduced at the (BBV) baryon-baryon-(vector-meson) vertex. The PPV vertex is taken to be pointlike. The various values for the remaining g's and α are then adjusted for a best fit to the data.

We consider the following question. Using values for $g_{\rho NN}$ and $g_{\omega NN}$ of comparable magnitude to those determined from various NN scattering analysis, can one obtain a reasonable fit to the low-energy KN data? Since the other BBV vertex parameters are less well established and tensor couplings are not included, comparison is done for the ρNN and ωNN vertices. In Table II we list the results of a search on the coupling constants for various values of α. Comparison with the available data is shown in Fig. 5 (and for the threshold branching ratios in Table I) using the "best fit" parameters for $\alpha=3$ GeV/c.

We note that it is remarkable that such a surprisingly good fit is obtained with so simple a model using (almost) pointlike meson-baryon vertex functions. Only ρ exchange has been included to describe the $\Sigma\pi\to\Sigma\pi$ scattering channel. Although low-energy theorems state that this should be the leading diagram, the data are quite constricting and one might expect the necessity of higher-order processes. From NN analyses, $g_V^2/4\pi$ for the ρNN vertex ranges in value between 2.0 and 4.0. From Table II it is seen that for a comparable ρNN coupling constant large values of α are necessary. From NN analyses (Ref. 23), α should be around 1.4 GeV/c. This difference may be the result of excluding higher-order

TABLE II. Best fit vertex coupling constants for different values of the form factor range parameter α. The coupling constants are defined in Eq. (11); the last column lists the χ^2 per data point for all the data (resonance, threshold, branching ratios, and scattering data).

Form factor range parameter	Coupling constants					
α (GeV)	$\frac{g^2_{\rho NN}}{4\pi}$	$\frac{g^2_{\omega NN}}{4\pi}$	$\frac{g^2_{K^*\Sigma N}}{4\pi}$	$\frac{g^2_{K^*\Lambda N}}{4\pi}$	$\frac{g^2_{\rho\Sigma\Sigma}}{4\pi}$	$\frac{\chi^2}{N}$
1.5	12.5	2.5	9.2	11.1	1.1	2.2
2.0	7.4	1.1	4.3	5.7	0.78	1.9
3.0	4.0	0.7	2.6	3.6	0.54	1.5
4.0	2.0	1.6	1.8	3.3	0.57	1.6

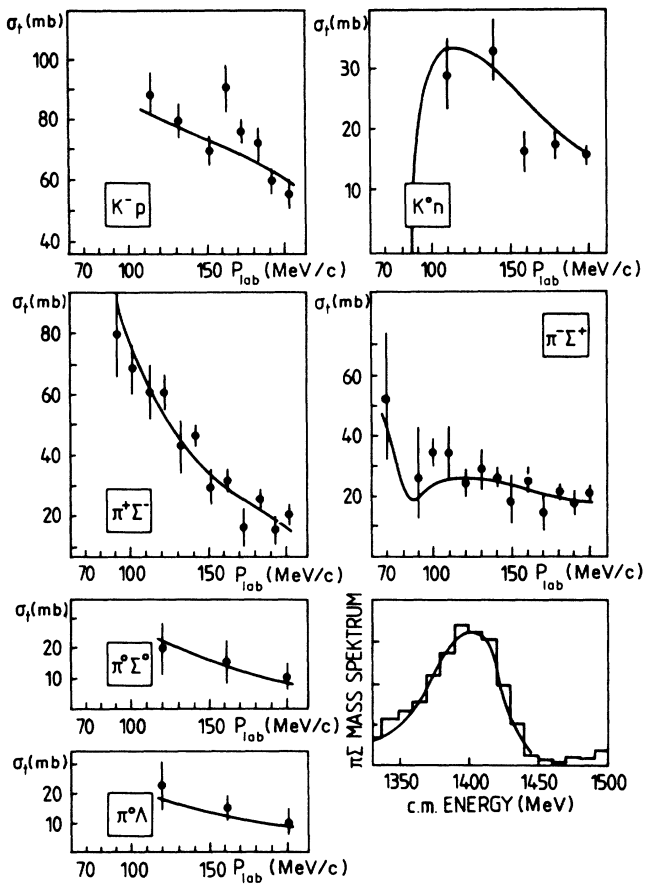

FIG. 5. Comparison with the low-energy data using the vector-meson exchange potential derived from Eq. (11). The parameter values for this fit are best fit values for $\alpha=3.0$ GeV/c given in Table II.

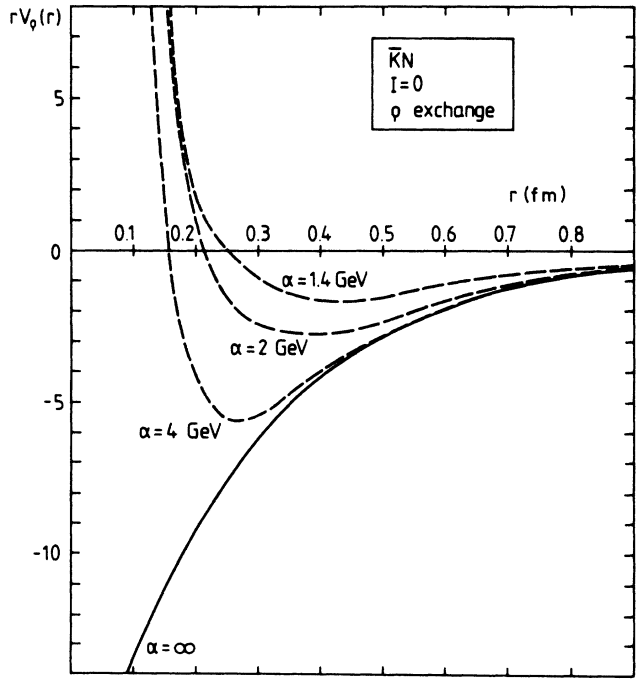

FIG. 6. Plot of the $\bar{K}N$ potential $V_\rho(r)$ in the $I=0$ channel due to ρ exchange for different vertex form factor ranges α; a value of $g^2_{\rho NN}/4\pi=3$ was used for demonstration.

processes. The reason for the larger cutoff α can be understood from the plot of the $\bar{K}N$ potential due to ρ exchange shown in Fig. 6. A form factor with $\alpha=1.4$ GeV/c produces effectively a short-range repulsion in the $\bar{K}N$ system. In order to provide sufficient attraction to form the resonance at 1405 MeV and produce enough charge exchange to raise the branching ratio γ to 2.36, an attractive potential is required from the ρ exchange. These coupling constants should be regarded as effective ones, and the value $\alpha=3$ GeV/c may be a consequence of the simplicity of the model. If $g^T_{\rho NN}/g^V_{\rho NN}$ were taken to be less than 6, then a much smaller value for α would produce a satisfactory fit to the data. In particular, the effective $\omega_8 NN$ coupling required by the fit is quite small. It may actually reflect the combined effect of ω exchange and the isoscalar part of higher-order processes. The next most important contributions would be the box diagrams shown in Fig. 7. These would contribute to both isoscalar and isovector exchange. The isovector component is attractive and would affect the ρ exchange parameters. The magnitude of these box diagrams is under consideration, as well as the effect of the $K\Xi$ channel which should be seen in the same context.

The scattering lengths obtained from the various potential fits are typically $a_0=-1.3+1.7i$ fm and $a_1=0.5+0.4i$ fm. They are similar to those found in Ref. 18. Closely related to the scattering lengths is the K^-p atomic $1s$ level shift. The K^-p atomic $1s$ level shift was calculated with the three meson-exchange potentials listed in Table I using the methods of Ref. 17. For these potentials, the shifts were -380 eV, which agree with values for the scattering length obtained with K-matrix parametrizations.[3] These values are, however, in disagreement with the K^-p atom experiments, but not with a different interpretation of these data given in Ref. 24.

VI. CONCLUSIONS

We have applied a separable potential and a meson-exchange potential model to the low-energy KN system

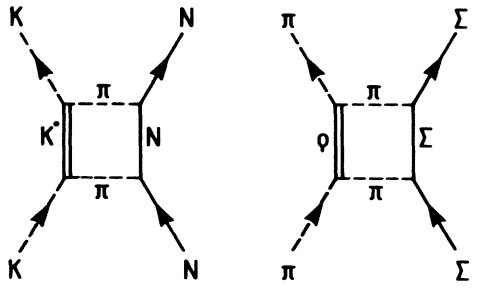

FIG. 7. Some box diagrams which would contribute to low-energy s-wave KN and $\Sigma\pi$ scattering.

and examined the degree of SU(3) symmetry breaking and the values of the various coupling constants necessary for a satisfactory fit to the available data. At threshold we have included only the less controversial threshold branching ratios for K^-p decay. We find that this data places tight constraints on potential model parameters. Any analysis which attempts to interpret the nature of the resonance at 1405 MeV or fit the K^-p 1s atomic level shift data needs to include this source of information.

Acceptable fits to all the data were obtained within the limits of expected SU(3) symmetry breaking, namely 25 percent. In a simple meson-exchange picture an excellent fit to the data was obtained with coupling parameters which are in rough agreement with similar analysis on the NN system, but with larger cutoff parameters in the vertex form factors. In conclusion, the low-energy data examined here are consistent with a quasi-bound-state picture of the $\Lambda(1405)$ generated by a t-channel potential. The experimental value for the 1s atomic shift is not compatible with these results, but would be in agreement with the interpretation of Ref. 24.

ACKNOWLEDGMENTS

We would like to thank Y. Fujiwara and M. Schaden for many useful discussions and remarks on this work. A special thanks is given to R. Büttgen and K. Holinde for help on the meson-exchange model of the interaction. We are grateful to John Durso, C. Fayard, and T. Mizutani for a careful reading of the manuscript and many helpful comments. This work was supported in part by the Bundeministerium für Forschung und Technologie (BMFT), under Grant No. MEP 0234 REA, and by Deutsche Forschungsgemeinschaft, under Grant No. We 655/9-1,2.

APPENDIX A: AN INTEGRAL RELATION

For the simple separable potential ansatz of Eq. (1), it is necessary to evaluate integrals of the form

$$I(E)=\int \frac{v^2(p)p^2dp}{E-E(p)+i\epsilon} , \tag{A1}$$

the determination of the scattering amplitude, and all other properties of the system. For the particular choice of $v(p)=\alpha/\alpha^2+p^2$ and $E-E(p)=(k_E^2-p^2)/2\mu$, which we use as the nonrelativistic propagator, Eq. (A1) becomes

$$\begin{aligned} I(E)&=2\mu\int_0^\infty \left[\frac{\alpha}{\alpha^2+p^2}\right]^2 \frac{p^2dp}{k_E^2-p^2+i\epsilon} \\ &=\mu\int_{-\infty}^{\infty} \left[\frac{\alpha}{\alpha^2+p^2}\right]^2 \frac{p^2dp}{k_E^2-p^2+i\epsilon} . \end{aligned} \tag{A2}$$

This integral is readily evaluated by closing the contour in the upper (or lower) half plane. For $k_E^2>0$, the integrand has poles at $\pm i\alpha$, and $\pm k_E$, and for $k_E^2<0$, all poles are on the imaginary axis. One obtains

$$I(E)=\begin{cases} \dfrac{\pi\mu\alpha}{2}\left[\dfrac{1}{\alpha^2+k_E^2}\right]\left[\dfrac{k_E^2-\alpha^2}{k_E^2+\alpha^2}\right]-i\pi\mu k_E\left[\dfrac{\alpha}{\alpha^2+k_E^2}\right]^2 & (k_E^2>0) \\ -\dfrac{\pi\mu\alpha}{2}\left[\dfrac{1}{\alpha+|k_E|}\right]^2 & (k_E^2<0) . \end{cases} \tag{A3}$$

APPENDIX B: VECTOR-MESON EXCHANGE POTENTIAL

A nonrelativistic limit of the vector-meson exchange graph, Fig. 8, can be carried out in a similar manner as done in Ref. 22 for the nucleon-nucleon interaction. Neglecting form factors, the matrix element represented by the graph in Fig. 8 is given in the center-of-mass system by

$$\mathcal{M}=i\bar{u}(p')\left[g_V\gamma^\mu+g_T\frac{i\sigma^{\mu\nu}q_\nu}{2M}\right]u(p)\frac{(k_u+k'_\mu)}{2\sqrt{\omega_k\omega_{k'}}}\frac{g}{\mathbf{q}^2+m_V^2} \tag{B1}$$

with $q_\mu=p'_\mu-p_\mu$, where g_V and g_T are the vector and tensor coupling constants. Here k_μ is the kaon momentum and $\omega_k=(k^2+m_K^2)^{1/2}$. Inserting the plane-wave spinors

$$u(p)=\left[\frac{E+M}{2M}\right]^{1/2}\begin{bmatrix}\chi \\ \dfrac{\boldsymbol{\sigma}\cdot\mathbf{p}}{E+M}\chi\end{bmatrix} ,$$

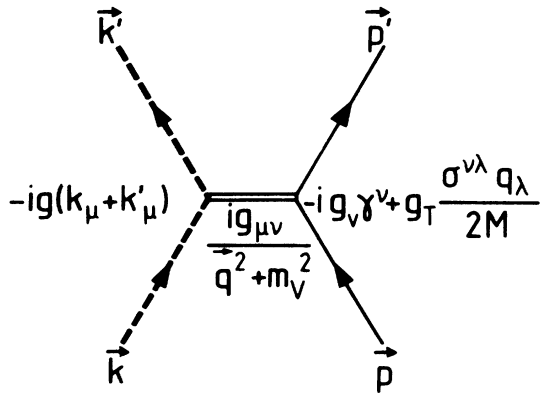

FIG. 8. Vector-meson exchange graph for the meson-baryon interaction. The isospin dependence is suppressed. The kinematical variables apply to ρ and ω exchange for which the initial and final particles are the same. Extension to K^* exchange is straightforward.

one obtains to order p^2/M^2 for ρ and ω exchange (dropping the isospin dependence for the moment):

$$\mathcal{M}=\frac{ig}{q^2+m_V^2}\left\{g_V\left[1+\frac{m_k+2M}{2M^2m_k}\left[\mathbf{K}^2+\frac{i}{2}\boldsymbol{\sigma}\cdot\mathbf{K}\times\mathbf{q}\right]\right]+g_T\left[-\frac{q^2}{4M^2}+\frac{m_k+M}{M^2m_k}\frac{i}{2}\boldsymbol{\sigma}\cdot\mathbf{K}\times\mathbf{q}\right]\right\}, \tag{B2}$$

where $\mathbf{K}$ is defined as $(\mathbf{p}+\mathbf{p})/2$. From this matrix element we construct a local potential by excluding the $\mathbf{K}^2$ terms. The $\boldsymbol{\sigma}\cdot(\mathbf{K}\times\mathbf{q})$ piece transforms to an $\mathbf{L}\cdot\mathbf{S}$ interaction in coordinate space which does not contribute in the s-wave channel. For our application, therefore, the appropriate nonrelativistic local reduction of the exchange graph of Fig. 3 leads to ρ- and ω-meson exchange potentials:

$$V_\omega(q^2)=\frac{-g}{q^2+m_V^2}\left[g_V^\omega-g_T^\omega\frac{q^2}{4M^2}\right]F(q^2)\,,$$
$$V_\rho(q^2)=\frac{g}{q^2+m_V^2}\left[g_V^\rho-g_T^\rho\frac{q^2}{4M^2}\right]F(q^2)\boldsymbol{\tau}_m\cdot\boldsymbol{\tau}_B\,, \tag{B3}$$

with the inclusion of the form factor $F(q^2)$ associated with the vertices. Here $\boldsymbol{\tau}_m$ and $\boldsymbol{\tau}_B$ refer to the meson and baryon isospins. For simplicity we use here $F(q^2)=(\alpha^2-m_v^2)/(\alpha^2+q^2)$ corresponding to a monopole form factor for the BBV vertex only. The K^* exchange potential for $\underline{KN\to\pi\Sigma}$ has an additional $(m_\pi+m_K)/(2\sqrt{m_\pi m_K})$ factor in the approximation that $M=\frac{1}{2}(M_\Sigma+M_N)$ is taken as the average of the Σ and nucleon masses.

*Present address: California State Polytechnic University at Pomona, Pomona, CA 91768.

[1]R. H. Dalitz, J. McGinley, C. Belyea, and S. Anthony, *Proceedings of the International Conference on Hypernuclear and Kaon Physics, Heidelberg, 1982* (Max-Plank-Institut für Kernphysik, Heidelberg, 1982), p. 201.
[2]E. M. Ross and G. Shaw, Ann. Phys. (N.Y.) **9**, 391 (1960); B. Martin and M. Sakitt, Phys. Rev. **183**, 1345 (1969).
[3]A. D. Martin, Nucl. Phys. **B179**, 33 (1981).
[4]M. Alberg, E. M. Henley, and L. Wilets, Ann. Phys. (N.Y.) **96**, 43 (1976); E. M. Henley, M. A. Alberg, and L. Wilets, Nukleonika **25**, 567 (1980).
[5]R. H. Landau, Phys. Rev. C **28**, 1324 (1983).
[6]A. Deloff and J. Law, Phys. Rev. C **20**, 1597 (1979); K. S. Kumar, Y. Nogami, W. van Dijk, and D. Kiang, Z. Phys. A **304**, 301 (1980).
[7]J. Law, M. J. Turner, and R. C. Barrett, Phys. Rev. C **35**, 305 (1987).
[8]For a discussion of this problem see D. Kiang, K. S. Kumar, Y. Nogami, and W. van Dijk, Phys. Rev. C **30**, 1638 (1984).
[9]J. Schnick and R. H. Landau, Phys. Rev. Lett. **58**, 1719 (1987).
[10]R. Nowak *et al.*, Nucl. Phys. **B139**, 61 (1978).
[11]D. Tovee *et al.*, Nucl. Phys. **B33**, 493 (1971).
[12]M. Sakett, T. B. Day, R. G. Glasser, N. Seeman, J. Friedman, W. E. Humphrey, and R. R. Ross, Phys. Rev. **139B**, 719 (1965).
[13]J. K. Kim, Columbia University Report **149**, 1966.
[14]W. E. Humphrey and R. R. Ross, Phys. Rev. **127**, 1305 (1962).
[15]D. Evans, J. V. Major, E. Rondio, J. A. Zakrzewski, J. E. Conboy, D. J. Miller, and T. Tymeiniecka, J. Phys. G **9**, 885 (1983).
[16]R. H. Dalitz and S. F. Tuan, Ann. Phys. (N.Y.) **10**, 307 (1960).
[17]P. B. Siegel, Z. Phys. A **328**, 239 (1987).
[18]E. A. Veit, B. K. Jennings, A. W. Thomas, and R. C. Barrett, Phys. Rev. D **31**, 1033 (1985).
[19]R. H. Dalitz, T.-C. Wong, and G. Rajasekaran, Phys. Rev. **153**, 1617 (1967).
[20]R. Hemingway, Nucl. Phys. **B253**, 742 (1985).
[21]K. S. Kumar and Y. Nogami, Phys. Rev. D **21**, 1834 (1980).
[22]R. Machleidt, K. Holinde, and Ch. Elster, Phys. Rep. **149**, 1 (1987).
[23]*Compilation of Coupling Constants and Low-Energy Parameters,* Nucl. Phys. **B216**, 277 (1983).
[24]H. H. Brouwer, J. W. de Maag, and L. P. Kok, Z. Phys. A **318**, 1 (1984).